



An anisotropic stellar fluid configuration with vanishing complexity

J. Andrade^{1,a} , D. Santana^{2,b}

¹ Escuela de Física y Matemática, Escuela Superior Politécnica de Chimborazo, (ESPOCH), Riobamba, Ecuador

² Escuela Superior Politécnica de Chimborazo, (ESPOCH), Riobamba, Ecuador

Received: 29 March 2023 / Accepted: 8 June 2023

© The Author(s) 2023

Abstract In this work, we construct a new stellar model in the regime of anisotropic fluid pressure using the concept of vanishing complexity for spherically symmetric fluid distributions (Herrera in Phys Rev D 97:044010, 2018) and a convenient ansatz in order to close the Einstein's field equations. The resulting model fulfills the fundamental physical acceptability stellar conditions for a specific set of compactness factor. The stability and its response against fluctuations in the matter sector is also investigated.

1 Introduction

In 1915, Einstein published his famous work on the General Theory of Relativity, which changed completely our view and understanding of the structure of space and time in the universe. The concepts related to this theory are realized in the Einstein's Field Equations (EFE), which describe how gravity arises from the curvature of space-time in the presence of matter or radiation. Since then, several works have been devoted to studying these equations and the construction of a wide range of models for describing phenomena from the solar system to cosmological scales. Thus, Schwarzschild [1] obtained the first EFE solution describing the space-time in the interior and exterior of a compact uniform-density sphere, and ever since, the modeling of relativistic stellar compact objects has moved from the regime of toy models to sophisticated, realistic stellar structures. For example, it is worth mentioning the seminal work of Tolman [2] in obtaining exact solutions of EFE for static fluid spheres and the pioneering work of Bowers and Liang [3] where the local anisotropy for static, and spherically symmetric distribution of matter is analysed. In this context, researchers have concentrated

on the formation and properties of these stellar structures, which are commonly used to refer to white dwarfs, neutron stars, and black holes. Thus, despite the fact that the complete nature of interactions inside of these stellar compact objects is still unknown, several models are published in order to characterize compact stellar structures.

Researchers consider both isotropic and anisotropic pressures on the relativistic fluid that supports the compact objects in order to develop models that can describe their main characteristics. To first approximation the local pressure isotropy can be considered a valid assumption in the study of stellar compact objects, however, it is known that many physical processes can produce deviations from isotropy and/or local anisotropy fluctuations in pressure that may be caused by a large variety of physical phenomena, especially in compact objects. Theoretical studies on more realistic stellar models in [4] show that nuclear matter may be locally anisotropic at very high densities. According to these views, the radial pressure may not be equal to the tangential pressure in massive stellar objects. Some of the research in this regard is reported in [5–12]. Additionally, it has been found strong evidence suggesting that for certain ranges of density, a large number of physical phenomena can cause local anisotropy and must therefore be considered in order to describe more realistic models. For example, one possible source of anisotropy is related to the intense magnetic fields observed in compact objects such as white dwarf stars, neutrons or magnetized quark stars [13–15], pion and meson condensations [16], exotic phase transitions [17] and others phenomena are extensively investigated in [18–22].

Even so, a recent result in [23] shows that any realistic physical process of the type expected in stellar evolution always tends to produce pressure anisotropy due to the presence of dissipation, energy density inhomogeneities, and shear. As a result, any final stage of a dynamical regime in the evolution of a star should exhibit pressure anisotropy. Con-

^a e-mail: julio.andrade@esepoch.edu.ec (corresponding author)

^b e-mail: diego.santana@esepoch.edu.ec

sequently, radial and tangential pressures become unequal, and the concept of local anisotropy inevitable emerges in the study of realistic compact stellar models [24–27].

It is worth noting that the problem of obtaining exact EFE solutions for static and spherically symmetric space-times supported by anisotropic fluid includes solving a robust system of coupled differential equations. The problem is that there are only three independent EFE, but five unknown quantities: two metric functions, the energy density, the radial and tangential pressures (matter sector). This issue has been addressed over time by employing widely successful strategies for obtaining precise EFE solutions [28–38]. Even exact solutions of the EFE for anisotropic fluid distribution on the background of a pseudo-spheroidal or paraboloidal space-times have been obtained in [39–43]. And for example, recently, the polytropic equation of state was used for developing models for compact objects with anisotropic polytropes [11,44,45], as well as modified polytropic equations of state are used to obtain anisotropic stellar models in [46,47], which result versatile in the way to describe several applications in astrophysics such as white dwarfs, neutron stars or Fermi fluids. Furthermore, it is worth noticing that in the Ref. [48] a novel approach to integrate the Lane–Emden equations for relativistic anisotropic polytropes is presented.

Particularly, in this work we obtain a new interior solution of EFE in the anisotropic regime of pressure as a result of the using as an extra condition the idea complexity for static self-gravitating spheres proposed by Herrera [49] and a convenient ansatz for the radial metric potential λ . This idea of complexity for the self-gravitating system has been widely accepted and used; it arises from the existence of a structure scalar called complexity factor Y_{TF} that contains information about the matter content of the fluid distribution. Specifically, this factor depends on pressure anisotropy and energy inhomogeneity. It is worth mentioning the case of the called “vanishing complexity”, where $Y_{TF} = 0$, which can be reached when both pressure anisotropy and energy inhomogeneity vanish, which pertains to the simplest case. When pressure anisotropy and energy inhomogeneity cancel out, another more fascinating scenario emerges.

This idea of complexity for self-gravitating spheres has been used as an extra condition to close the EFE in order to obtain new stellar models. Thus, we can mention several works where this definition has been used; for example, recently, anisotropic solutions of EFE describing embedding Class I compact stars have been obtained by using a vanishing complexity factor condition in the context of the Gravitational Decoupling approach (GD) (see Refs. [50–55] for details about GD approach) [56], as well as the construction of an anisotropic generalization of the Buchdahl static stellar model by implementing the method of GD via extended minimal geometric deformation and further requiring vanishing complexity in [57]. Also, it is worth mentioning that

the role of GD on isotropization and complexity of self-gravitating systems under the complete geometric deformation approach and the role of complexity on self-gravitating compact stars under GD have been studied in [58,59], respectively. Even this definition has been used for the construction of new stellar models in the framework of alternative theories of gravity (see, for example, the Refs. [60–73]); for example, the vanishing complexity and gravitational decoupling approach have been used to investigate a spherically symmetric anisotropic solution in $f(Q)$ gravity theory for the first time recently in [74].

In this work, we also use the definition of vanishing complexity for self-gravitating spheres in order to close the resulting EFE. The obtained solution is regular and meets all physical plausibility conditions, and its stability is also investigated. It is worth mentioning that the number of interior solutions in the regime of anisotropic fluid with vanishing complexity is reduced nowadays; therefore, new models with these characteristics are important in the field of theoretical astrophysics, and therefore the relevance of obtaining this kind of new solutions is well established.

The paper has been organized as follows: Sect. 2 is dedicated to reviewing briefly the EFE for anisotropic fluid distribution, in Sect. 3 we introduce and review the idea of complexity for self-gravitating fluid spheres, in Sect. 4 we obtain a new stellar model with the aim of vanishing complexity and a convenient choice of ansatz on radial metric potential, in Sect. 5 we briefly review the fundamental stellar physical acceptability conditions for a realistic stellar compact object, while in Sect. 6, contains a physical analysis of the model. Finally, in Sect. 7, we draw some conclusions about our work.

2 Einstein field equations for anisotropic fluid distributions

The Einstein field equations (EFE) for vanishing cosmological constant are

$$G_{\mu\nu} \equiv R_{\mu\nu} - \frac{1}{2}g_{\mu\nu}R = \kappa T_{\mu\nu}, \quad (1)$$

where $R_{\mu\nu}$ the Ricci tensor, R is the curvature scalar, $T_{\mu\nu}$ is the energy–momentum tensor and $\kappa = \frac{8\pi G}{c^4}$. Now, in order to model a star, we must use the space-time of a static self-gravitating sphere provided by the metric

$$ds^2 = e^\nu dt^2 - e^\lambda dr^2 - r^2(d\theta^2 + \sin^2\theta d\phi^2), \quad (2)$$

where ν and λ are functions (called as metric potentials) that depend only on the radial coordinate r . In such sense in the co moving frame the physical interior of the self-gravitating object can be modelled as an relativistic anisotropic fluid given by a density energy ρ , radial pressure p_r and tangential pressure p_t . So in this way the energy–momentum tensor $T_{\mu\nu}$

is represented by

$$T_{\mu\nu} = (\rho + p_t)u_\mu u_\nu - p_t g_{\mu\nu} + (p_r - p_t)s_\mu s_\nu, \quad (3)$$

whose components (ρ, p_r, p_t, p_t) are known as the matter sector of the interior solution and

$$u^\mu = (e^{-\nu/2}, 0, 0, 0), \quad (4)$$

is the four velocity of the fluid and s^μ another quantity define as

$$s^\mu = (0, e^{-\nu/2}, 0, 0), \quad (5)$$

with the properties $s^\mu u_\mu = 0$ and $s^\mu s_\mu = -1$.

So if one uses the information of Eqs. (2) and (3) in EFE (1), one arrives at

$$8\pi\rho = \frac{1}{r^2} + e^{-\lambda} \left(\frac{\lambda'}{r} - \frac{1}{r^2} \right), \quad (6)$$

$$8\pi p_r = -\frac{1}{r^2} + e^{-\lambda} \left(\frac{\nu'}{r} + \frac{1}{r^2} \right), \quad (7)$$

$$8\pi p_t = \frac{e^{-\lambda}}{4} \left(2\nu'' + \nu'^2 - \lambda'\nu' + 2\frac{\nu' - \lambda'}{r} \right), \quad (8)$$

where primes denote differentiation with respect to the radial coordinate r , and we assume the geometric units $G = c = 1$. Note that Eqs. (6)–(8) constitutes a set of three differentials equations with five unknown quantities: $\{\nu, \mu\}$ (metric potentials) and $\{\rho, p_r, p_t\}$. So in order to solve this system, it is necessary to use two extra conditions, which usually can be geometrical relations (for example, the Karmakar condition [75]), equations of state (EoS) that relate the physical quantities of matter sector (for example, the polytropic equation of state, the Van der Waals equation of state, etc. [76–79]) and others. In particular, in this work we use the idea of complexity for static self-gravitating fluid spheres of Herrera [49] and a convenient choice of an ansatz for the radial metric potential λ in order to obtain a new interior solution for EFE.

Furthermore, the contracted Bianchi identities ensure that the Einstein tensor is divergence-free. Then, by the Eq. (1), we can derive the covariant conservation of the energy-momentum tensor as follows:

$$\nabla_\mu T^{\mu\nu} = 0, \quad (9)$$

which explicitly gives us the generalized Tolman–Oppenheimer–Volkoff (TOV) equation for anisotropic fluid

$$\frac{dp_r}{dr} = -\frac{\nu'}{2}(\rho + p_r) - \frac{2\pi}{r}, \quad (10)$$

with $\pi \equiv p_r - p_t$. If one uses the definition of mass function given by

$$R_{232}^3 = 1 - e^{-\lambda} = \frac{2m}{r}, \quad (11)$$

or equivalently

$$m = 4\pi \int_0^r \tilde{r}^2 \rho(\tilde{r}) d\tilde{r} \quad (12)$$

the TOV can be expressed as

$$\frac{dp_r}{dr} = -\frac{(m + 4\pi r^3 p_r)}{r(r - 2m)} (\rho + p_r) - \frac{2\pi}{r}, \quad (13)$$

which accounts for the hydrostatic balance of the fluid within the interstellar object. Note that the pressure gradient is balanced by a gravitational term and a term that includes the local anisotropy distribution.

3 Complexity of self-gravitating spheres

The concept of complexity varies greatly depending on the subject of study, particularly; in this work, we shall use a definition of complexity for static and spherically symmetric self-gravitational systems that was recently proposed by Herrera [49, 80, 81] in the context of the general theory of relativity. This definition replaces the fundamental idea of probability distribution that appears in the definition of “imbalance” and information by the energy density of the fluid distribution (see [82]). And likewise, this definition replaces certain previous definitions of complexity for self-gravitating spheres that considered only the energy density of the fluid, ignoring the other components of the energy–momentum tensor that describes the interior of the star from the point of view of general theory of relativity.

This definition is based on the structure of the fluid distribution (i.e., fluid inhomogeneity and pressure anisotropy), in such a way that the simplest system is the one with perfect fluid distribution, and that more complex systems are those that vary from this fundamental system, especially those that deviate from the regular pattern of constant energy density and pressure isotropy.

Specifically, such a definition surges from the existence of a structure scalar (denoted by Y_{TF}) that is connected to the orthogonal splitting of the Riemann tensor [83, 84] in static and spherically symmetric space-times (for the first time, such a scalar and others were thoroughly examined in [85]). The Riemann tensor can be expressed through the Weyl tensor $C_{\alpha\beta\mu}^\nu$, the Ricci tensor $R_{\mu\nu}$ and the curvature scalar R in the following way:

$$R_{\alpha\beta\mu}^\nu = C_{\alpha\beta\mu}^\nu + \frac{1}{2} R_\beta^\nu g_{\alpha\mu} - \frac{1}{2} R_{\alpha\beta} \delta_\mu^\nu + \frac{1}{2} R_{\alpha\mu} \delta_\beta^\nu - \frac{1}{2} R_\mu^\nu g_{\alpha\beta} - \frac{1}{6} R (\delta_\nu^\beta g_{\alpha\mu} - g_{\alpha\beta} \delta_\nu^\mu), \quad (14)$$

and by other hand, we can only express the Weyl tensor in terms of its electric part because the magnetic part vanishes

in the spherically symmetric case:

$$E_{\mu\nu} = C_{\mu\gamma\nu\delta} u^\gamma u^\delta. \quad (15)$$

It should be noted that $E_{\mu\nu}$ can also be written as

$$E_{\mu\nu} = E \left(s_\mu s_\nu + \frac{1}{3} h_{\mu\nu} \right), \quad (16)$$

with

$$E = -\frac{e^{-\lambda}}{4} \left(v'' + \frac{v'^2 - \lambda' v'}{2} - \frac{v' - \lambda'}{r} + \frac{2(1 - e^\lambda)}{r^2} \right), \quad (17)$$

$$h_\nu^\mu = \delta_\nu^\mu - u^\mu u_\nu, \quad (18)$$

having the properties for $E_{\mu\nu}$:

$$E_\mu^\mu = 0, \quad E_{\mu\nu} = E_{(\mu\nu)}, \quad E_{\mu\nu} u^\mu = 0. \quad (19)$$

It is now possible to show that the Riemann tensor can be expressed using tensors (see [84] for details) as

$$Y_{\mu\nu} = R_{\mu\gamma\nu\delta} u^\gamma u^\delta \quad (20)$$

$$Z_{\mu\nu} = {}^*R_{\mu\gamma\nu\delta} u^\gamma u^\delta \quad (21)$$

$$X_{\mu\nu} = {}^*R_{\mu\gamma\nu\delta}^* u^\gamma u^\delta \quad (22)$$

in what is called the orthogonal splitting of the Riemann tensor. Here $*$ denotes the dual tensor, i.e., $R_{\mu\gamma\nu\delta}^* = \frac{1}{2} \eta_{\epsilon\sigma\gamma\delta} R_{\mu\nu}^{\epsilon\sigma}$ and $\eta_{\mu\nu\lambda\rho}$ corresponds to the Levi-Civita tensor.

$T_{\mu\nu}$ can be expressed in a particularly useful manner so that after some manipulations, namely

$$Y_{\mu\nu} = \frac{4}{3} \pi (\rho + 3p) h_{\mu\nu} + 4\pi \Pi_{\mu\nu} + E_{\mu\nu}, \quad (23)$$

$$Z_{\mu\nu} = 0, \quad (24)$$

and

$$X_{\mu\nu} = \frac{8}{3} \pi \rho h_{\mu\nu} + 4\pi \Pi_{\mu\nu} - E_{\mu\nu}, \quad (25)$$

with

$$\Pi_\nu^\mu = \Pi \left(s_\nu^\mu s_\nu + \frac{1}{3} h_\nu^\mu \right) \quad (26)$$

$$P = \frac{p_r + 2p_t}{3}. \quad (27)$$

Thus, from the tensors $X_{\mu\nu}$ and $Y_{\mu\nu}$ is possible to define four structure scalar functions in the following way:

$$X_T = 8\pi \rho \quad (28)$$

$$X_{TF} = 4\pi \Pi - E \quad (29)$$

$$Y_T = 4\pi (\rho + 4p_r - 2\Pi), \quad (30)$$

and

$$Y_{TF} = 4\pi \Pi + E. \quad (31)$$

As a result of the preceding, X_{TF} and Y_{TF} determine the local anisotropy of pressure:

$$X_{TF} + Y_{TF} = 8\pi \Pi. \quad (32)$$

Also, it is possible to express Y_{TF} in terms of energy density inhomogeneity and system local anisotropy by

$$Y_{TF} = 8\pi \Pi - \frac{4\pi}{r^3} \int_0^r \tilde{r}^3 \rho' d\tilde{r}. \quad (33)$$

This scalar captures the concept of complexity since it measures the relationship between the inhomogeneity in the energy density and the pressure anisotropy of a static and spherically symmetric self-gravitational system.

Additionally, it can be demonstrated that (33) permits one to express the Tolman mass as

$$m_T = (m_T)_\Sigma \left(\frac{r}{r_\Sigma} \right)^3 + r^3 \int_r^{r_\Sigma} \frac{e^{(v+\lambda)/2}}{\tilde{r}} Y_{TF} d\tilde{r}, \quad (34)$$

where the subscript Σ indicates that the quantity is evaluated on the boundary surface Σ . Equation (34) shows that this scalar includes all the alterations caused by the energy density inhomogeneity and the anisotropy of the pressure on the active gravitational mass, namely, the Tolman mass, which is a combination of its value for a zero-complexity system and two other terms related to energy density inhomogeneity and pressure anisotropy, respectively. It can be viewed as a convincing justification to define the complexity factor by means of this scalar. Thus, this scalar represents an appropriate parameter that characterizes the complexity of self-gravitating static spheres because, first and foremost, it is based on a structure scalar (which is critical because it ensures that this characteristic is founded on a quantity that is invariant for any observer) that contains all physical parameters of the matter sector of the interior of the self-gravitating sphere, and, more specifically, it is dependent on inhomogeneity in the energy density and anisotropy in the pressure.

Now, it is worth noticing that if one uses the EFE (6)–(8) in (33) arrives at

$$Y_{TF} = \frac{e^{-\lambda}}{4r} [v' (2 + r\lambda' - rv') - 2rv''], \quad (35)$$

which represents an alternative method of calculating Y_{TF} using knowledge of the space-time within the stellar compact source.

Equation (33), in particular, has been used as a state equation to construct a limited number of new interior solutions for static self-gravitating spheres [56–59, 86–95]. For example, it is significant to note that the vanishing complexity criterion, namely, when $Y_{TF} = 0$, is met not only in the most straightforward instances of isotropic and homogeneous sys-

tems, but also in the situations where

$$\Pi = \frac{1}{2r^3} \int_0^r \tilde{r}^3 \rho' d\tilde{r}, \quad (36)$$

namely, in the scenarios where the pressure anisotropy and energy inhomogeneity cancel each other.

The system of EFE can be closed using Eq. (36) as a complementing condition because it reflects a non-local equation of state (three interesting formalisms to construct solutions with such a characteristic have been developed recently in [91, 96, 97]).

4 New stellar model

The vanishing complexity condition, $Y_{TF} = 0$, yields the differential equation shown below

$$v'' - \left(\frac{1}{r} + \frac{\lambda'}{2} \right) v' + \frac{1}{2} v'^2 = 0, \quad (37)$$

for which is necessary the information of the radial metric potential λ in order to obtain v . So in this work we propose an ansatz for the radial metric potential given by

$$e^{-\lambda} = \frac{A}{A + Br^2}, \quad (38)$$

where A and B are constants. In principle, we propose this ansatz only because we have tested it and it is suitable for us to find a regular and adequate new solution to the EFE, and it is not associated with any particular physical motivation. In particular, one can associate our ansatz with the particular case of the well-behaved metric function corresponding to the Finch–Skea solution [56, 98] given by $e^{-\lambda} = \frac{1}{1+Lr^2}$ where $L = \frac{B}{A}$.

Therefore, using this ansatz in (37) we arrive at

$$e^v = e^{c_2} \left((A + Br^2)^{3/2} + 6Bc_1 \right)^2, \quad (39)$$

with c_1 and c_2 integration constants.

Now, using the metric potentials (38)–(39) in EFE, we obtain the matter sector given by

$$\rho = \frac{B(3A + Br^2)}{8\pi(A + Br^2)^2}, \quad (40)$$

$$p_r = \frac{B}{8\pi} \left[\frac{6A}{\sqrt{A + Br^2} \left((A + Br^2)^{3/2} + 6Bc_1 \right)} - \frac{1}{A + Br^2} \right], \quad (41)$$

$$\Pi = -\frac{B^2 r^2}{8\pi (A + Br^2)^2}, \quad (42)$$

with $A + Br^2 > 0$ and $c_1 \neq -\frac{(A + Br^2)^{3/2}}{6B}$.

Furthermore, by employing the matching conditions (see C6. in the following section), we have

$$c_1 = -\frac{BR^2 - 5A}{6B} \sqrt{A + BR^2} \quad (43)$$

$$e^{c_2} = \frac{R - 2M}{36A^2 R (A + BR^2)} \quad (44)$$

$$A = \frac{BR^3 - 2BMR^2}{2M}, \quad (45)$$

with $A + BR^2 > 0$.

5 Physical acceptability conditions

The fundamental physical requirements necessary to any interior solution can describe a realistic stellar compact object are (see Ref. [99] for a detailed discussion of these conditions):

- C1. The metrics e^v and $e^{-\lambda}$ should be finite and regular in the interior of a stellar compact object; e^v should be a monotonously increasing function of radial coordinate r , and $e^{-\lambda}$ should be a monotonously decreasing function. Furthermore, $e^{v(0)} = \text{constant}$ and $e^{-\lambda(0)} = 1$.
- C2. The matter sector given by the density energy ρ , radial pressure p_r and transversal pressure p_t should be positive and regular inside the compact stellar object. They should be monotonously decreasing functions of radial coordinate r , with their maximum values at the center. Also, $p_t(r) > p_r(r)$ inside the star, with the exception of the center, where $p_t(0) = p_r(0)$. Moreover, the radial pressure should vanish at the boundary of the star.
- C3. The Dominant Energy Condition (DEC): $\rho - p_r \geq 0$ and $\rho - p_t \geq 0$ should be fulfilled $\forall r, r \leq R$. Also, it is desirable that even the strong energy condition (SEC) $\rho \geq p_r + 2p_t$ is satisfied. Obviously, the latter encompasses DEC.
- C4. The redshift function $z(r) = g_{tt}^{-1/2}(r) - 1$ should decrease outward, and its value at the surface $z(r = R)$ is less than the universal bound for solutions satisfying the DEC, namely $z_{\text{bound}} = 5.211$ [100].
- C5. The stability of the stellar object requires that the speed of sound should be less than the speed of light, $c = 1$, which leads $0 \leq v_r^2 = \frac{dp_r}{d\rho} \leq 1$ and $0 \leq v_t^2 = \frac{dp_t}{d\rho} \leq 1$ inside of a stellar compact object.
- C6. At the boundary of the stellar compact object ($r = R$), the metric components e^v and $e^{-\lambda}$ should match continuously with the Schwarzschild exterior solution, namely

$$e^v|_{r=r_\Sigma} = e^{-\lambda}|_{r=r_\Sigma} = 1 - \frac{2M}{R}, \quad (46)$$

where M and $r_\Sigma = R$ are the total mass and radius of the star, respectively.

As also is necessary that

$$p_r(r = R) = 0 \quad (47)$$

since the exterior of the star in this case is considered to be empty.

6 Physical analysis

In this section, we analyse the physical acceptance of the stellar model obtained in this work. In this sense, we have checked that the behavior of the whole model given by Eqs. (38)–(45) is regular within the set of compactness factors of $0.4023 \leq u = \frac{M}{R} \leq 0.4104$.

6.1 Metrics

It is noticeable that *C1* of the previous section is fulfilled for the model in Figs. 1 and 2, as well, we can notice that e^v is a monotonously increasing function of r and $e^{-\lambda}$ is a monotonously decreasing function of the same variable r . So the space-time within the stellar compact object behaves as expected.

6.2 Matter sector

In Figs. 3, 4, and 5, the behavior of the matter sector of the solution is presented. We can note from these figures that condition *C2* is fulfilled. Furthermore, from Fig. 6, we can note that $\Delta = -\Pi > 0$, and the radial and tangential pressures are equal in the center of the stellar object, which is absolutely necessary in order to maintain certain stability of the stellar object.

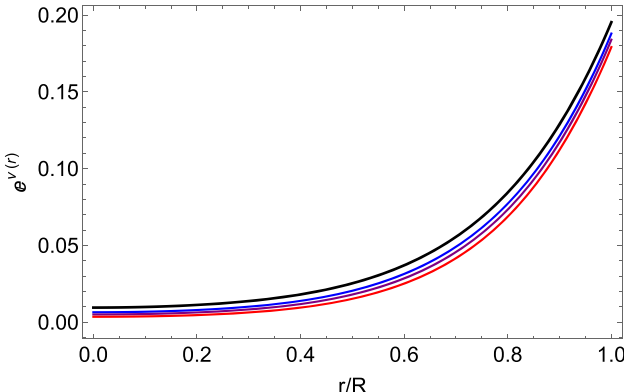


Fig. 1 e^v for compactness factors of 0.4023 (black line), 0.406 (blue line), 0.408 (purple line), 0.4104 (red line)

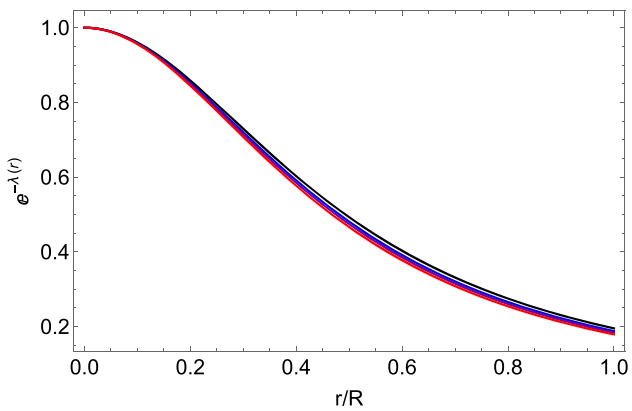


Fig. 2 $e^{-\lambda}$ for compactness factors of 0.4023 (black line), 0.406 (blue line), 0.408 (purple line), 0.4104 (red line)

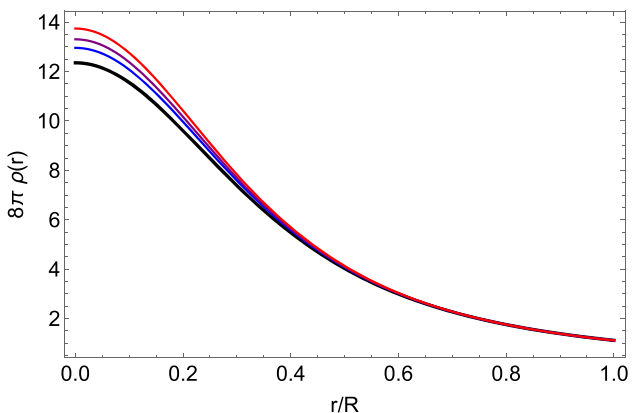


Fig. 3 ρ for compactness factors of 0.4023 (black line), 0.406 (blue line), 0.408 (purple line), 0.4104 (red line)

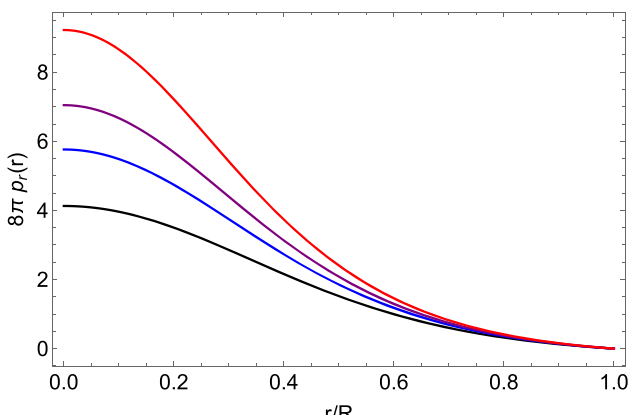


Fig. 4 p_r for compactness factors of 0.4023 (black line), 0.406 (blue line), 0.408 (purple line), 0.4104 (red line)

6.3 Energy conditions and causality

On the other hand, it is also necessary to show that our model should satisfy the dominant energy condition given by *C3* in order to affirm that this matter sector belongs to an

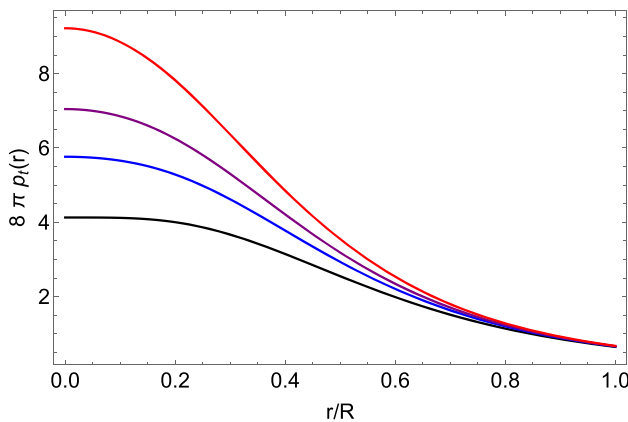


Fig. 5 p_t for compactness factors of 0.4023 (black line), 0.406 (blue line), 0.408 (purple line), 0.4104 (red line)

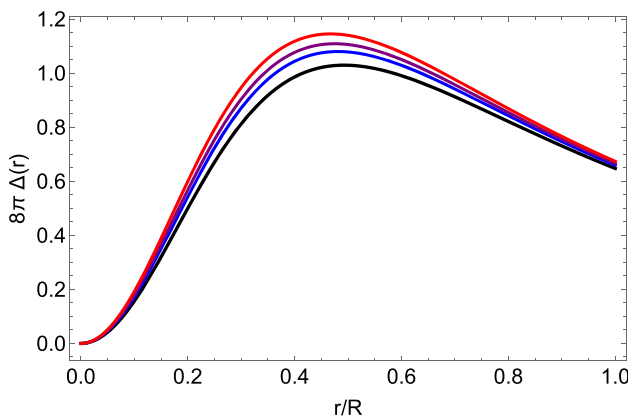


Fig. 6 $p_t - p_r$ for compactness factors of 0.4023 (black line), 0.406 (blue line), 0.408 (purple line), 0.4104 (red line)

acceptable physical energy–momentum source. This is effectively observed in Figs. 7 and 8. However, we have checked that the model does not fulfill the Strong Energy Condition (SEC) described in C3 for the compactness parameters $0.35 < u = M/R$ (see Fig. 9). Based on the foregoing, we can conclude that our model can explain realistic stars from an energy standpoint because it should obey either of the two energy conditions (DEC or SEC) [99–102].

Moreover, in Figs. 10 and 11 the profiles of sound velocities inside of the star are shown. It is noticeable that these velocities do not surpass the limit value of light velocity in vacuum that in this case is taken as $c = 1$. However, these results are interesting since their profiles are not monotonous functions of the radial coordinate r .

6.4 Redshift

In Fig. 12, the redshift z is plotted. In this figure, we can observe that the redshift is a monotonously decreasing function of the radial coordinate r , having its maximum value at the center of the stellar compact object. Also, it is noticeable

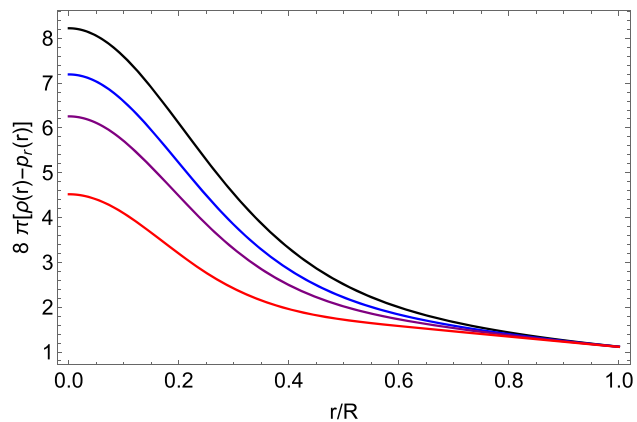


Fig. 7 $\rho - p_r$ for compactness factors of 0.4023 (black line), 0.406 (blue line), 0.408 (purple line), 0.4104 (red line)

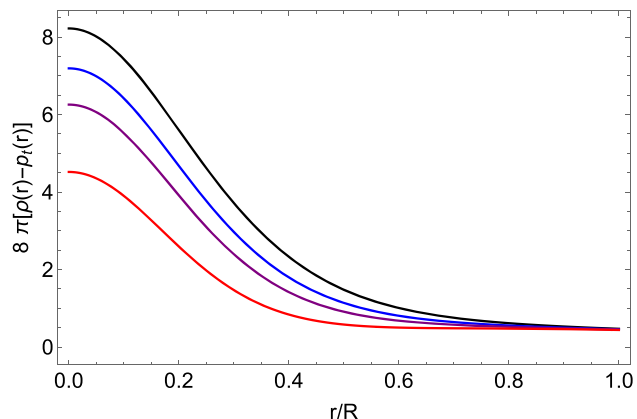


Fig. 8 $\rho - p_t$ for compactness factors of 0.4023 (black line), 0.406 (blue line), 0.408 (purple line), 0.4104 (red line)

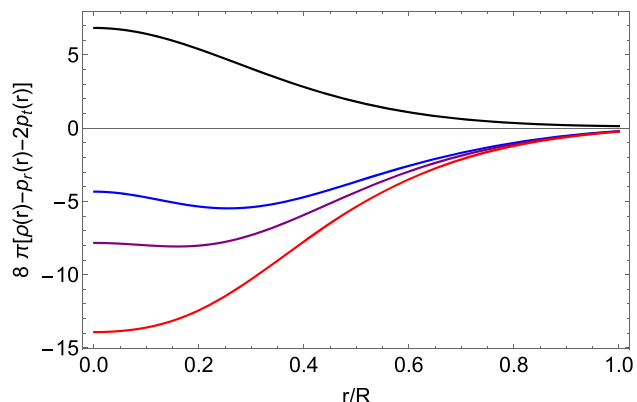


Fig. 9 $\rho - p_r - 2p_t$ for compactness factors of 0.35 (green line), 0.4023 (black line), 0.406 (blue line), 0.408 (purple line), 0.4104 (red line)

that the surface redshift value is below the universal bound of $z_{\text{bound}} = 5.211$.

We have checked that for the obtained solution fulfills the fundamental physical conditions for those compactness parameters mentioned before. However, since the anisotropy

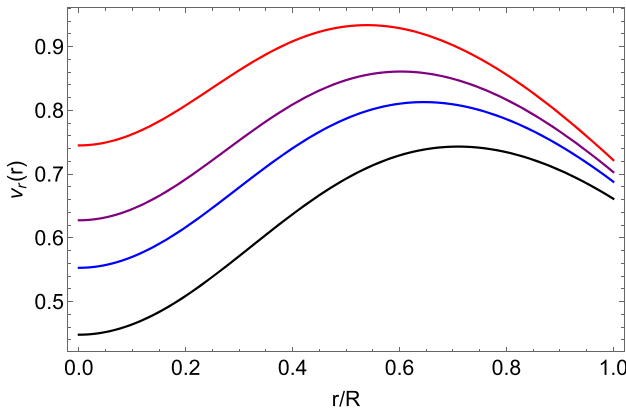


Fig. 10 v_r for compactness factors of 0.4023 (black line), 0.406 (blue line), 0.408 (purple line), 0.4104 (red line)

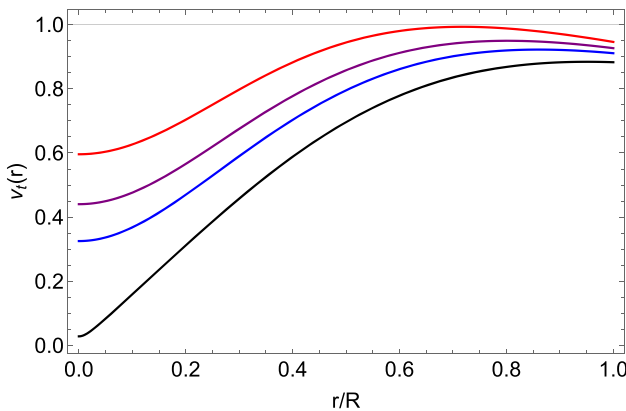


Fig. 11 v_t for compactness factors of 0.4023 (black line), 0.406 (blue line), 0.408 (purple line), 0.4104 (red line)

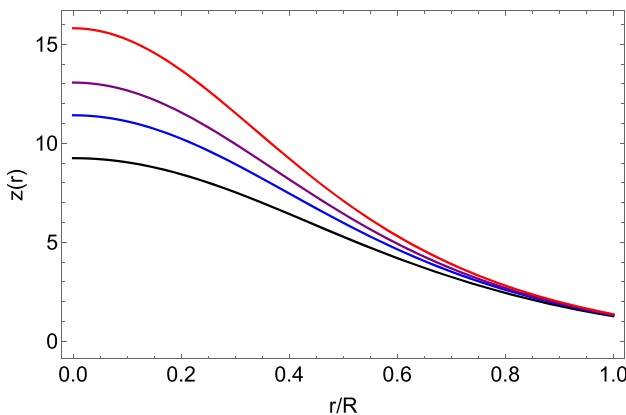


Fig. 12 z for compactness factors of 0.4023 (black line), 0.406 (blue line), 0.408 (purple line), 0.4104 (red line)

Δ and sound velocities have a non-monotonous decreasing behavior inside the stellar compact object, it is possible that the model is unstable. As a result, in this work, we go a step further and investigate the stability of the new solution in the next four subsections.

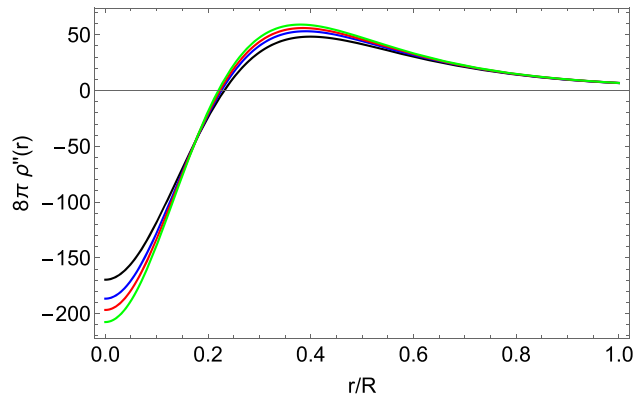


Fig. 13 ρ'' for compactness factors of 0.4023 (black line), 0.406 (blue line), 0.408 (red line), 0.4104 (green line)

6.5 Stability against convection criterion

The stability of a spherical stellar compact object to convection implies the buoyancy principle: any fluid element pushed downward must float back to its original position [103–105]. This implies that in any hydrostatic matter configuration, pressure and energy density must decrease outwards. Any fluid that supports a self-gravitating sphere should satisfy this principle in order to remain stable during convection, then in such sense it was demonstrated in [106] that if the energy density of any fluid distribution is such that

$$\rho'' \leq 0, \quad (48)$$

then effectively it fluid distribution fulfills such principle.

Thus, in order to study this condition, in Fig. 13, we show the profile of ρ'' for our model. From this figure, it is observable that the model fulfills this stability condition in the inner regions of the star, while the outer regions are unstable. To some extent, it could be argued that the outer layers can tolerate this instability while the inner layers can not; to some extent, this could be tolerated. But nevertheless, if the behavior were the opposite, that is, if Eq. (48) is true for the outer layers and not for the inner ones, this would imply that each element of mass tends towards the center of the star, potentially causing a collapse.

6.6 Stability against gravitational collapse criterion

To investigate the resistance of the model to collapse, it is necessary to examine the behavior of the adiabatic index Γ in the radial direction given by

$$\Gamma = \frac{\rho + p_r}{p_r} \frac{dp_r}{d\rho}, \quad (49)$$

which should satisfy

$$\Gamma_{crit} \leq \Gamma \quad (50)$$

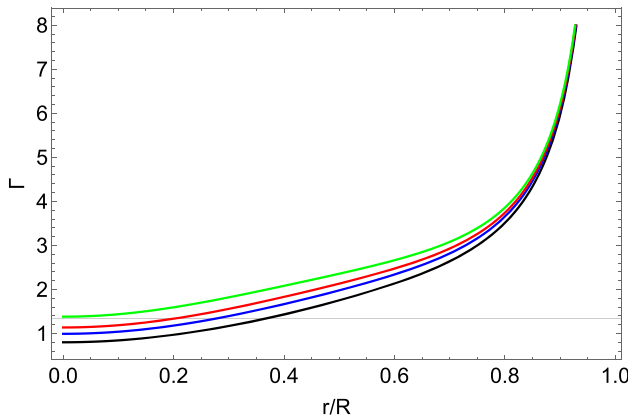


Fig. 14 Γ for compactness factors of 0.4023 (black line), 0.406 (blue line), 0.408 (red line), 0.4104 (green line)

with

$$\Gamma_{crit} = \frac{4}{3} + \frac{19}{21}u. \quad (51)$$

This is because a spherically symmetric system is only affected in the radial direction against eventual gravitational collapse in the presence of local anisotropies.

The aforementioned relationship given by Eq. (50) accounts for relativistic changes to the adiabatic index, which can cause instabilities within the star. The second term on the right side of Eq. (51) represents relativistic corrections to the Newtonian perfect fluid and anisotropy contribution. This stability condition (50) thus applies to any relativistic compact object supported by an anisotropic fluid. Furthermore, this condition asserts the existence of a critical value for the adiabatic index Γ_{crit} . This critical value is determined by the amplitude of the Lagrangian displacement from equilibrium and $u = M/R$ is the compactness factor (see Refs. [107–109] for a more in-depth discussion of this point).

In this sense, we have plotted the behavior of Γ in function of radial coordinate r in Fig. 14. We have checked that the model presents instability against collapse for the compactness factors shown in the caption of Fig. 14.

6.7 Harrison–Zeldovich–Novikov stability criterion

Also known as the “static stability criterion”, it establishes that any relativistic stellar fluid will be stable and static under radial perturbations if the mass of the system is increasing as a function of its central energy density ρ_0 , namely, $\frac{dM}{d\rho_0} > 0$. The total mass as a function of its central density for this model is

$$M = \frac{4\pi\rho_0R^2}{3 + 8\pi\rho_0R^2}, \quad (52)$$

from which we obtain that

$$\frac{dM}{d\rho_0} = \frac{12\pi R^3}{(3 + 8\pi\rho R^2)^2},$$

which is of course positive since $R > 0$. This means that the new model satisfy the static stability criterion. Therefore the anisotropic compact objects described by our new model are stable. However, they are unstable when their internal gases undergo an adiabatic process related to gravitational collapse because the stability against gravitational collapse criterion is not satisfied, which is the first point associated with extreme changes in gravitational force inside stars.

The above result leads us to analyse the behavior of the matter sector of these models against small perturbations in the next subsection.

6.8 Gravitational cracking criterion

In this section we study the behavior of the fluid distribution of our model just after its departure from equilibrium, when total non-vanishing radial forces of different signs appear within the system. This analysis is based on the idea of cracking produced in a spherical fluid distribution, which was first developed by Herrera in 1992 [110] and then fine tuned in later works [111–113]. The analysis focuses on studying when the radial force in the interior of stellar compact object is directed inward in the inner part of the sphere and reverses its sign beyond some value of the radial coordinate, we say there is a cracking, even if only after the fluid deviates from equilibrium. In the opposite case, when the force is directed outward in the inner part and changes sign in the outer part, we shall say that there is an overturning.

It is important to mention that cracking is closely related to the problem of compact object structure formation, but only at time scales smaller than or equal to the hydrostatic time scale [114–116]. In such a sense, the cracking analysis is just take a photography of the state of total radial force within the stellar compact object when it departs from equilibrium. Likewise, it should be clarified that the appearance of fractures directly and drastically affects the future structure and evolution of the compact object.

So to carry out this analysis, it is necessary to note that the TOV (10) or (13) can be rewritten as

$$\mathcal{R} = \frac{dp_r}{dr} + \frac{(m + 4\pi r^3 p_r)}{r(r - 2m)}(\rho + p_r) - \frac{2\Delta}{r}, \quad (53)$$

where \mathcal{R} is the total radial force within the stellar compact object per unit of volume on each fluid element. When the stellar system is in hydrostatic equilibrium, this total force \mathcal{R} is null, however, when the system is facing some disturbance, this force can deviate from that value. So it is interesting to study those scenarios where these deviations occur.

In such a sense, we shall assume that the perturbation is done for the whole matter sector of the stellar model except that the radial pressure remains unperturbed, namely, we have to change or perturb the parameters of the model in such way that $\mathcal{R} \neq 0$. The idea is if the model has the parameters $\{\alpha, \beta\}$ the “perturbed” TOV can be written as (up to first order)

$$\hat{\mathcal{R}} = \frac{\partial \hat{\mathcal{R}}}{\partial \alpha} \delta\alpha + \frac{\partial \hat{\mathcal{R}}}{\partial \beta} \delta\beta + \mathcal{O}(\delta\alpha^2, \delta\beta^2). \quad (54)$$

Now, if the system experiments a cracking or overturning is necessary that at some point $\hat{\mathcal{R}}$ changes of sign in some interior point of the stellar object, which is traduced in the existence of some real root for $\hat{\mathcal{R}} = 0$. Thus it can be seen how the existence of some real value \mathcal{E} such as $\delta\beta = -\mathcal{E}\delta\alpha$, and moreover that

$$\mathcal{E} = \frac{\partial \tilde{\mathcal{R}}/\partial \tilde{\alpha}|_{\beta, \alpha}}{\partial \tilde{\mathcal{R}}/\partial \tilde{\beta}|_{\beta, \alpha}}. \quad (55)$$

To apply this analysis to our model, we must first define the dimensionless quantities listed below

$$\alpha = A \quad (56)$$

$$\beta = BR^2 \quad (57)$$

$$x = \frac{r}{R} \quad (58)$$

in terms of which we can write

$$\rho = \frac{\beta(3\alpha + \beta x^2)}{8\pi R^2 (\alpha + \beta x^2)^2} \quad (59)$$

$$p_r = -\frac{1 - \frac{\alpha \left(\frac{6\beta x^2 \sqrt{\alpha + \beta x^2}}{5\alpha \sqrt{\alpha + \beta} - \beta \sqrt{\alpha + \beta} + (\alpha + \beta x^2)^{3/2}} + 1 \right)}{\alpha + \beta x^2}}{8\pi R^2 x^2} \quad (60)$$

$$\Pi = -\frac{\beta^2 x^2}{8\pi R^2 (\alpha + \beta x^2)^2} \quad (61)$$

$$m = \frac{\beta R x^3}{2\alpha + 2\beta x^2}, \quad (62)$$

for which we also use the condition (43).

Now, we proceed to perturb the matter sector through the variation of the parameters $\{\alpha, \beta\}$

$$\alpha \rightarrow \tilde{\alpha} = \alpha + \delta\alpha, \quad (63)$$

$$\beta \rightarrow \tilde{\beta} = \beta + \delta\beta, \quad (64)$$

where the tilde indicates that the quantity has been perturbed. The total radial force, on a fluid element, in terms of $\{\tilde{\alpha}, \tilde{\beta}\}$ results in

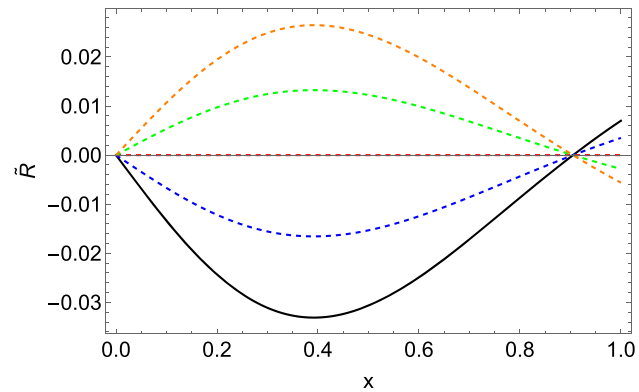


Fig. 15 $\tilde{\mathcal{R}}$ for $\beta = 0.7$, $\alpha = 1$, $\mathcal{E} = -1.7$ (black line), $\mathcal{E} = -1.2$ (blue line), $\mathcal{E} = -0.7$ (red line), $\mathcal{E} = -0.3$ (green line) and $\mathcal{E} = 0.5$ (orange line)

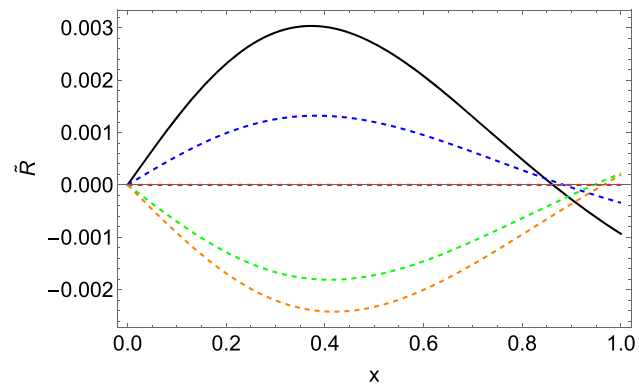


Fig. 16 $\tilde{\mathcal{R}}$ for $\beta = 0.7$, $\mathcal{E} = -0.7$, $\alpha = 0.90$ (black line), $\alpha = 0.95$ (blue line), $\alpha = 1.00$ (red line), $\alpha = 1.10$ (green line) and, $\alpha = 1.15$ (orange line)

$$\begin{aligned} \tilde{\mathcal{R}}(\alpha + \delta\alpha, \beta + \delta\beta, x) &= \tilde{\mathcal{R}}(\alpha, \beta, x) + \frac{\partial \tilde{\mathcal{R}}}{\partial \tilde{\alpha}}|_{\alpha, \beta} \delta\alpha \\ &+ \frac{\partial \tilde{\mathcal{R}}}{\partial \tilde{\beta}}|_{\beta, \alpha} \delta\beta + \mathcal{O}(\delta\alpha^2, \delta\beta^2), \end{aligned} \quad (65)$$

where the first term is zero given that it corresponds to the unperturbed values of $\tilde{\mathcal{R}}$. Of course, after perturbation, the TOV is different from zero, so the system is no longer in hydrostatic equilibrium. Note that if cracking (or overturning) occurs, $\tilde{\mathcal{R}}$ must have a zero in the interval $x \in (0, 1)$.

In Figs. 15, 16, and 17, we represent $\tilde{\mathcal{R}}$ as a function of x for different values of \mathcal{E} , α and β , respectively. For the realization of these figures we have taken into account the condition $A + BR^2 > 0$, which can be written as $\alpha + \beta > 0$. In Fig. 15, we show the profile of $\tilde{\mathcal{R}}$ with the values of $\beta = 0.7$ and $\alpha = 1$ and different values of \mathcal{E} . Note that for the value of $\mathcal{E} = -0.7$ the radial force is $\tilde{\mathcal{R}} = 0$ for every point inside the star, but for the lower values of \mathcal{E} the system experiments overturning and for the upper ones the fracture corresponds to cracking. Interestingly, the perturbed total radial

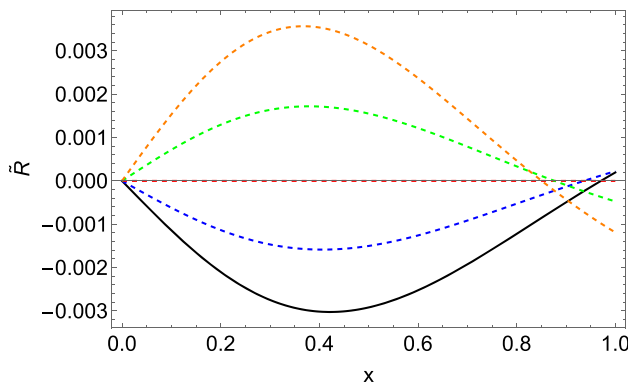


Fig. 17 \tilde{R} for $\alpha = 1.0$, $\Xi = -0.7$, $\beta = 0.60$ (black line), $\beta = 0.65$ (blue line), $\beta = 0.70$ (red line), $\beta = 0.75$ (green line) and $\beta = 0.80$ (orange line)

force experiments a kind of transition between scenarios with overturning to scenarios with cracking when the value of Ξ increases, and thus the radius where cracking/overturning occurs coincide for all the values of Ξ considered.

On the hand, in Fig. 16, the profile of \tilde{R} is shown for the values of $\beta = 0.7$, $\Xi = -0.7$ and different values of α . It is noticeable that under this configuration of parameters values the system experiments a transition between configurations with cracking to configurations with overturning when we increase the value of α . Note that the fracture (cracking or overturning) moves to inner shells with the reduction of α . Also, it is worth noting that there is a configuration (red line) where the system experiments the hydrostatic equilibrium, namely, in such case $\tilde{R} = 0$ inside of the stellar compact object.

In Fig. 17, instead, we plot the behavior of \tilde{R} for the parameter values of $\alpha = 1.0$, $\Xi = -0.7$ and for different values of β . We can observe that the system for this configuration can experiment a kind of transition between scenarios with overturning and scenarios with cracking when the β value is increased. Also, it is important to note that there is a configuration (red line) where $\tilde{R} = 0$. We can see that if β value increases, the fracture (overturning or cracking) moves to the inner shells of the stellar compact object.

In light of what has been mentioned before, we can conclude that the system can experience internal fracture (cracking or overturning) when it is subjected to small perturbations in its matter sector. If the value α of is increased, these fractures move to the outer regions, whereas β increasing causes the opposite behavior. Also, as shown in Figs. 15, 16 and 17, the stellar compact object can experiment transitions between scenarios with cracking and scenarios with overturning by varying the values of Ξ , α and β , respectively. It is worth also notice that there are configurations with hydrostatic equilibrium even after the perturbation action (see red lines in Figs. 15, 16 and 17).

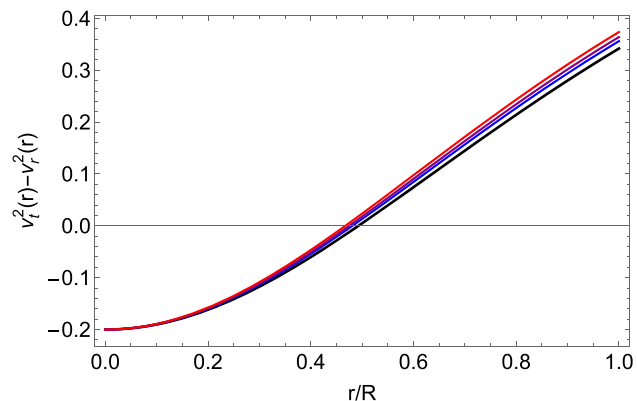


Fig. 18 $v_t^2 - v_r^2$ for compactness factors of 0.4023 (black line), 0.406 (blue line), 0.408 (purple line), 0.4104 (red line)

In addition, if one observes again the Fig. 6, namely, the behavior of the local anisotropy of stellar compact object can note that there is a region in $x = r/R \in (0.4; 0.5)$ where the anisotropy changes smoothly in its growth with respect to the radial variable r , which in certain measure approximately coincides with maximum values of the perturbed radial force \tilde{R} in Figs. 15, 16 and 17, demonstrating a link between the presence of local anisotropy and the formation of fracture (cracking or overturning) inside the stellar compact object. Furthermore, we can see from these figures that fractures inside stars tend to occur in the outer regions of the stellar compact object, while anisotropy decreases in these regions, which can be interpreted as showing how this descent of anisotropy in these outer regions can be related to the appearance of these fractures, which is consistent with the work [111], where it was shown that cracking results only if, in the process of perturbation leading to departure from equilibrium, the local anisotropy is perturbed, suggesting that fluctuations of local anisotropy may be crucial in the occurrence of cracking (see the works [117–119] where it is shown that anisotropy play an important role in the appearance of cracking).

Given the preceding results, it becomes vital to apply a basic condition founded by Abreu in [101] to determine zones of stability against gravitational cracking given by

$$-1 \leq v_t^2 - v_r^2 \leq 0. \quad (66)$$

In this way we plot the profile of $v_t^2 - v_r^2$ in the Fig. 18. We can observe that the condition (66) is satisfied by the inner shells of the star, namely, the inner shells are stable regions against gravitational cracking, and the outer regions are unstable regions, which corresponds to Figs. 15, 16, and 17 because the fractures appear precisely in these outer regions. Also, is worth mentioning that the transition between the stable and unstable regions in Fig. 18 is around at $x = r/R \in (0.4; 0.5)$, which corresponds to those regions where the local anisotropy undergoes a change in its growth with

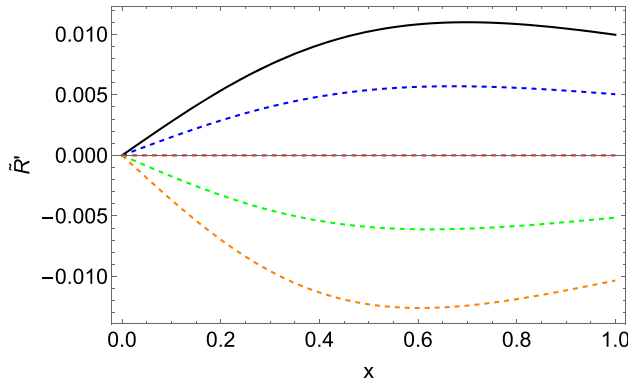


Fig. 19 \tilde{R}' for $\beta = 0.7$, $\alpha = 1$, $\mathcal{E} = -1.7$ (black line), $\mathcal{E} = -1.2$ (blue line), $\mathcal{E} = -0.7$ (red line), $\mathcal{E} = -0.3$ (green line) and $\mathcal{E} = 0.5$ (orange line)

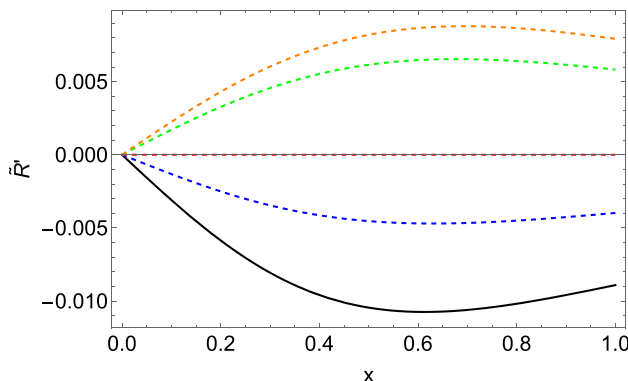


Fig. 20 \tilde{R}' for $\beta = 0.7$, $\mathcal{E} = -0.7$, $\alpha = 0.90$ (black line), $\alpha = 0.95$ (blue line), $\alpha = 1.00$ (red line), $\alpha = 1.10$ (green line) and $\alpha = 1.15$ (orange line)

respect to the radial variable r and with the maximum values of the perturbed radial force \tilde{R} . Namely, the outer regions are unstable when we add small perturbations in the matter sector of our model. Thus, this result reinforces the idea of the existence of direct relation between the presence of local anisotropy and the apparition of cracking inside the stellar compact object.

In order to avoid leaving only qualitative comments on the important role that local anisotropy plays in the appearance of fractures in the interior of the compact stellar object, we perform the same analysis but with the caveat that now we will consider the fluctuations over the entire material sector of the solution except for radial pressure and local anisotropy; that is, we consider the previous analysis but with the consideration that the radial pressure and the local anisotropy remain undisturbed. Thus, from these considerations, we have obtained the following Figs. 19, 20, and 21. Note that we have labelled the new radial force \tilde{R}' in order to differentiate it from \tilde{R} . The first that we note from these figures is that the total \tilde{R}' has the opposite sign with respect to \tilde{R} for the same configuration of parameters (see Figs. 15, 16, and 17),

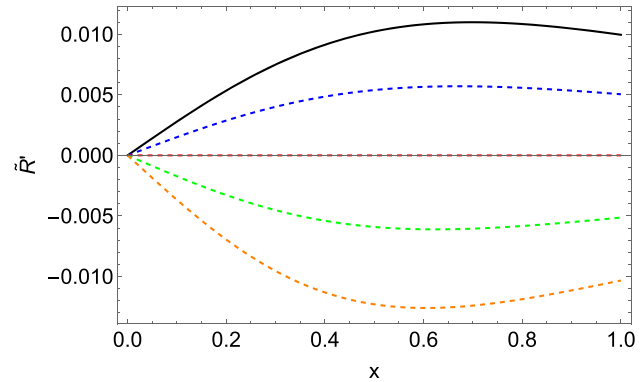


Fig. 21 \tilde{R}' for $\alpha = 1.0$, $\mathcal{E} = -0.7$, $\beta = 0.60$ (black line), $\beta = 0.65$ (blue line), $\beta = 0.70$ (red line), $\beta = 0.75$ (green line) and $\beta = 0.80$ (orange line)

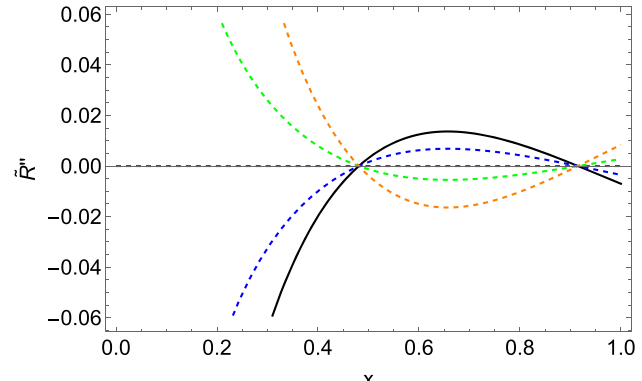


Fig. 22 \tilde{R}'' for $\beta = 0.7$, $\alpha = 1$, $\mathcal{E} = -1.7$ (black line), $\mathcal{E} = -1.2$ (blue line), $\mathcal{E} = -0.7$ (red line), $\mathcal{E} = -0.3$ (green line) and $\mathcal{E} = 0.5$ (orange line)

but also and most importantly that \tilde{R}' has not any fracture (cracking or overturning). Furthermore, we have checked that if the anisotropy function Δ is not considered in \tilde{R} a similar result is obtained also. Also note that the configurations with null total radial force \tilde{R} remain unchanged (red lines) in \tilde{R}' . So in this sense, we show that effectively the presence of local anisotropy or its fluctuations causes the presence of cracking inside the stellar object for our model, which is in accordance with previous works.

Now, since we have shown the model is unstable against gravitational collapse and stable about the Harrison–Zeldovich–Novikov stability criterion, it would seem interesting to observe what happens to this total radial force if we perturb it solely on its radial pressure. Therefore, we use the same analysis of cracking, but this time we only perturb the radial pressure, while the other physical quantities remain unchanged. In this case, we obtain Figs. 22, 23, and 24. In this case we labelled the resultant total radial force like \tilde{R}'' for distinguish from the previous ones. We notice that the total radial force shoots towards very high values as it approaches the center of the star, which can indicate that if we perturb the

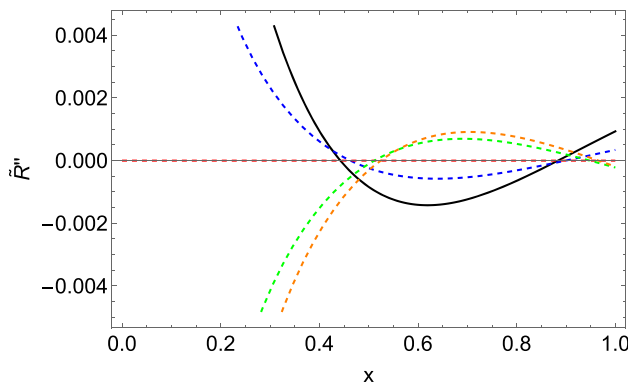


Fig. 23 \tilde{R}'' for $\beta = 0.7$, $E = -0.7$, $\alpha = 0.90$ (black line), $\alpha = 0.95$ (blue line), $\alpha = 1.00$ (red line), $\alpha = 1.10$ (green line) and, $\alpha = 1.15$ (orange line)

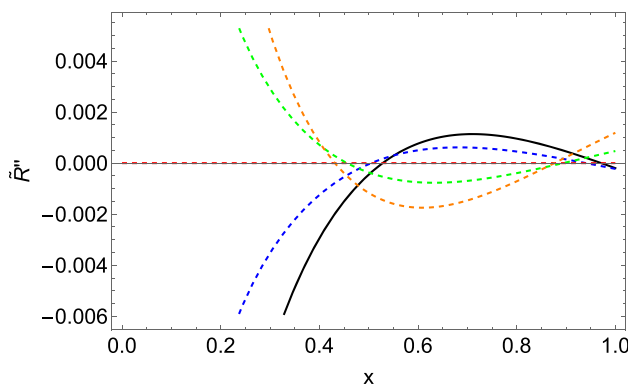


Fig. 24 \tilde{R}'' for $\alpha = 1.0$, $E = -0.7$, $\beta = 0.60$ (black line), $\beta = 0.65$ (blue line), $\beta = 0.70$ (red line), $\beta = 0.75$ (green line) and $\beta = 0.80$ (orange line)

total radial force just in the radial pressure a huge force in the direction of the stellar center is induced. At this point, we can associate this with the fact that this model is unstable against gravitational collapse since these small disturbances raise big distortions in the radial direction as causes of gravitational collapse. But, on the other side, the Harrison–Zeldovich–Novikov stability criterion is also satisfied; therefore, we can not affirm with all reliability that these great forces actually cause the gravitational collapse. Even one possibility can be that the huge forces generated by radial disturbances are big but finite, so in this sense, the stellar compact object can support these forces without breaking its static stability and does not collapse under radial disturbances. But since cracking only shows us the trend just when the hydrostatic equilibrium is broken and not beyond its evolution for sufficiently long times to know the final state of the star, we can not affirm whether these disturbances generate the collapse or not.

Also, it is interesting to note that the system also experiences fractures in regions further from the center of the star center and that the configurations with hydrostatic equi-

librium (red lines) remain stable despite the perturbations. Despite the great instability of this model, it is possible to find configurations where it is totally stable even under the action of disturbances in its matter sector, which is reinforced from the fact that the static stability criterion is fulfilled.

7 Conclusions

A new stellar model in the regime of anisotropic fluid has been developed. For such construction, we introduce a convenient ansatz for the radial metric component of the space-time of the system, and the temporal metric component was obtained using the well-established definition of vanishing complexity for self-gravitating spheres. After getting the static and spherically distributed space-time metric, we used it to obtain the matter sector. The physical behavior was analyzed, finding that the model satisfies the physical requirements to represent realistic stellar compact objects, in this sense, the whole physical conditions of Sect. 5 are fulfilled for a certain set of compactness factors of $0.4023 \leq u = \frac{M}{R} \leq 0.4104$.

On the other hand, the model is stable against convection in its inner regions but unstable in the outer regions of the stellar compact object. In this sense, it could be conjectured about the existence of a central core inside the star that does not allow the outermost layers of the star to collapse inside due to convective movement, which must be common due to the extreme conditions in temperature and densities inside a star. However, the model presents instability against gravitational collapse for the set of compactness parameters mentioned before. In such a sense, we can mention that the possible tendency to collapse in this case is not associated with the convective motion inside the stellar compact object. At the same time, we checked that the model satisfies the Harrison–Zeldovich–Novikov, which in a certain sense is opposed to instability with respect to gravitational collapse, so that it could be thought at first that the stars represented by this model have great stability with respect to their hydrostatic balance in the face of radial perturbations, but nevertheless, if they are very intense, there could be a possible collapse. In any case, we cannot affirm this with absolute certainty.

In this regard, the response of the model against small perturbations in its matter sector was analyzed in Sect. 6.8, and the gravitational cracking criterion proposed by L. Herrera was used. Namely, whenever the total non-vanishing radial force appearing after the perturbation goes out of hydrostatic equilibrium, having the possibilities that it is directed inward in the inner part of the sphere and change its direction at some r less than the radius of the star, and the opposite case named as overturning. We analyze specifically, the state of the system just after it departs from equilibrium. Firstly, we have evidence that the system experiments a type of tran-

sition between scenarios where the cracking is presented and scenarios where the overturning is presented with the variation of the parameters involved in the model, specifically the fracture point (cracking or overturning) appears in the inner regions of the star if the values of \mathcal{E} and β are increased, while the fracture appears in the outer regions with the increase of values of α , namely, the inner shells of the stellar compact object are stable against cracking and the outer ones are unstable.

It is also worth noting that the system can experiment with scenarios in which the total radial perturbed force $\tilde{\mathcal{R}}$ is equal to zero, i.e. scenarios in which the system is in equilibrium despite perturbations in the matter sector. As a result, we can argue that the presence of internal fractures is not required in all cases for this model, as there are scenarios or configurations with absolute hydrostatic equilibrium despite the action of the model's small perturbations in the matter sector. Moreover, we have shown explicitly the direct relation in the appearance of any fracture inside the stellar compact object with the presence of the local anisotropy and its fluctuations, namely, without these two characteristic our model is free of any internal fracture (cracking or overturning even when it is perturbed).

Thus, if the system only experiences fluctuations in its radial pressure, it causes a triggered increase in its total radial force directed to the center of the star, which we believe are scenarios associated with gravitational collapse in principle, but which could also be scenarios of high central density but static stability because the model responds to the Harrison–Zeldovich–Novikov stability criterion. In this sense, we are not sure that the appearance of these large forces can cause the collapse; in fact, there could be the possibility that these huge forces are compensated by the presence of local anisotropy if we also take into account the presence of disturbances in the entire material sector, and that the collapse can occur in extreme cases associated with a large adiabatic compression of the baryonic gas inside the star by huge gravitational forces. That is, we can not make a conclusive statement about whether these forces actually cause a gravitational collapse.

Also, it is worth mentioning the presence of fractures in the external parts of the compact object at the same time, which is to say that in addition to the apparition of huge forces directed to the center of the stellar compact object, there would be a dynamic in the external layers. These results mentioned before show us theoretically in a certain measure that there are a wide number of plausible physical processes giving rise to deviations from local isotropy, which take on relevance since the occurrence of these types of fracture has direct implications on the structure and evolution of the compact object at time scales that are smaller than or equal to the hydrostatic time scale and are associated with a wide number of physical processes that are present in a star, such as intense magnetic fields observed in compact objects, neu-

trino viscosity, exotic phase transitions, and the superposition of perfect fluids, among others. In any case, the appearance of these fractures can be speculated about and associated with the origin of several important stellar processes such as star quakes and gravitational collapse, the emergence of inner core fractures will undoubtedly change the conditions for outer mantle ejection in supernova events, as well as the occurrence of glitches and bursts of X-rays and gamma rays in neutron stars.

Data Availability Statement This manuscript has no associated data or the data will not be deposited. [Authors' comment: This is a theoretical work. No experimental data was used.]

Open Access This article is licensed under a Creative Commons Attribution 4.0 International License, which permits use, sharing, adaptation, distribution and reproduction in any medium or format, as long as you give appropriate credit to the original author(s) and the source, provide a link to the Creative Commons licence, and indicate if changes were made. The images or other third party material in this article are included in the article's Creative Commons licence, unless indicated otherwise in a credit line to the material. If material is not included in the article's Creative Commons licence and your intended use is not permitted by statutory regulation or exceeds the permitted use, you will need to obtain permission directly from the copyright holder. To view a copy of this licence, visit <http://creativecommons.org/licenses/by/4.0/>.

Funded by SCOAP³. SCOAP³ supports the goals of the International Year of Basic Sciences for Sustainable Development.

References

1. K. Schwarzschild, *Sitzungsber. deutsch. Akad. Wiss. Berlin, Kl. Math. Phys. Technik*, 189 (1916)
2. R.C. Tolman, *Phys. Rev.* **55**(4), 364 (1939)
3. R.L. Bowers, E.P.T. Liang, *Astrophys. J.* **188**, 657 (1974)
4. M. Ruderman, *Annu. Rev. Astron. Astrophys.* **10**, 427 (1972)
5. K. Dev, M. Gleiser, *Gen. Relativ. Gravit.* **34**, 1793 (2002)
6. M.K. Mak, P.N. Dobson, T. Harko, *Int. J. Mod. Phys. D* **11**, 207 (2002)
7. M.K. Mak, T. Harko, *Chin. J. Astron. Astrophys.* **2**, 248 (2002)
8. M. Chaisi, S.D. Maharaj, *Pramana J. Phys.* **66**, 609–614 (2006)
9. K. Komathiraj, S.D. Maharaj, *J. Math. Phys.* **48**, 042501 (2007)
10. K. Komathiraj, S.D. Maharaj, *Int. J. Mod. Phys. D* **16**, 1803 (2007)
11. S. Thirukkanesh, F.C. Ragel, *Pramana J. Phys.* **78**, 687 (2012)
12. S.K. Maurya, Y.K. Gupta, *Astrophys. Space Sci.* **344**, 243–251 (2013)
13. G.D. Schmidt, P.S. Schmidt, *Astrophys. J.* **448**, 305 (1995)
14. A. Putney, *Astrophys. J.* **451**, L67 (1995)
15. A.P. Martinez, R.G. Felipe, D.M. Paret, *Int. J. Mod. Phys. D* **19**, 1511 (2010)
16. R.F. Sawyer, *Phys. Rev. Lett.* **29**, 382 (1972)
17. R. Kippenhahn, A. Weigert, A. Weiss, *Stellar Structure and Evolution*, vol. 192 (Springer, Berlin, 1990)
18. L. Herrera, N.O. Santos, *Phys. Rep.* **286**, 53 (1997)
19. L. Herrera, G. Le Denmat, N.O. Santos, *Phys. Rev. D* **79**, 087505 (2009)
20. L. Herrera, G. Le Denmat, N.O. Santos, *Class. Quantum Gravity* **27**, 135017 (2010)
21. L. Herrera, G.L. Denmat, N.O. Santos, *Gen. Relativ. Gravit.* **44**, 1143 (2012)

22. S.K. Maurya, S.D. Maharaj, J. Kumar, A.K. Prasad, *Gen. Relativ. Gravit.* **51**, 1–28 (2019)

23. L. Herrera, *Phys. Rev. D* **101**, 104024 (2020)

24. L. Herrera, W. Barreto, *Phys. Rev. D* **88**, 084022 (2013)

25. L. Herrera, J. Ospino, A. Di Prisco, *Phys. Rev. D* **77**, 027502 (2008)

26. L. Herrera, W. Barreto, *Phys. Rev. D* **87**, 087303 (2013)

27. L. Herrera, A. Di Prisco, W. Barreto, J. Ospino, *Gen. Relativ. Gravit.* **46**, 1827 (2014)

28. D. Kramer, E. Herlt, M. MacCallum, H. Stephani, in *Exact Solutions of Einstein's Field Equations*, ed. by E. Schmutz (Cambridge University Press, Cambridge, 1979)

29. J. Bičák, Selected solutions of Einstein's field equations: their role in general relativity and astrophysics, in *Einstein's Field Equations and Their Physical Implications. Lecture Notes in Physics*, vol. 540, ed. by B.G. Schmidt (Springer, Berlin, 1999)

30. J.B. Griffiths, J. Podolský, *Exact Space-Times in Einstein's General Relativity* (Cambridge University Press, Cambridge, 2009)

31. S.K. Maurya, Y.K. Gupta, S. Ray et al., *Eur. Phys. J. C* **75**, 225 (2015)

32. S.K. Maurya, A. Banerjee, S. Hansraj, *Phys. Rev. D* **97**(4), 044022 (2018)

33. S.K. Maurya et al., *Phys. Rev. D* **99**(4), 044029 (2019)

34. Y.K. Gupta, S.K. Maurya, *Astrophys. Space Sci.* **331**(1), 135–144 (2011)

35. F. Tello-Ortiz, M. Malaver, A. Rincón et al., *Eur. Phys. J. C* **80**, 371 (2020)

36. K. Dev, M. Gleiser, *Gen. Relativ. Gravit.* **34**, 1793–1818 (2002)

37. M.K. Mak, T. Harko, *Proc. R. Soc. Lond. Ser. A. Math. Phys. Eng. Sci.* **430**(2030), 393–408 (2003). <https://doi.org/10.1098/rspa.2002.1014>

38. S.K. Maurya, Y.K. Gupta, B. Dayanandan, M.K. Jasim, A. Al-Jamel, *Int. J. Mod. Phys. D* **26**(02), 1750002 (2017)

39. R. Tikekar, V.O. Thomas, *Pramana J. Phys.* **52**, 237–244 (1999)

40. V.O. Thomas, D.M. Pandya, *Astrophys. Space Sci.* **360**, 59 (2015). <https://doi.org/10.1007/s10509-015-2573-3>

41. B.S. Ratanpal, V.O. Thomas, D.M. Pandya, *Astrophys. Space Sci.* **361**, 65 (2016)

42. V.O. Thomas, D.M. Pandya, *Eur. Phys. J. A* **53**, 120 (2017)

43. D.M. Pandya, V.O. Thomas, *Can. J. Phys.* **97**, 337 (2019)

44. S.A. Mardan, A. Asif, I. Noureen, *Eur. Phys. J. Plus* **134**, 242 (2019)

45. G. Abellán, P. Bargueño, E. Contreras, E. Fuenmayor, *Int. J. Mod. Phys. D* **29**(12), 2050082 (2020)

46. K.N. Singh et al., *Phys. Scr.* **95**, 115301 (2020)

47. P. León, E. Fuenmayor, E. Contreras, *Phys. Rev. D* **107**(6), 064010 (2023)

48. D. Santana, E. Fuenmayor, E. Contreras, *Eur. Phys. J. C* **82**, 703 (2022)

49. L. Herrera, *Phys. Rev. D* **97**, 044010 (2018)

50. J. Ovalle, *Mod. Phys. Lett. A* **23**, 3247 (2008)

51. J. Ovalle, Braneworld stars: anisotropy minimally projected onto the brane, *Gravitation and Astrophysics (ICGA9)*, pp. 173–182 (2010). https://doi.org/10.1142/9789814307673_0017

52. J. Ovalle, *Phys. Rev. D* **95**, 104019 (2017)

53. J. Ovalle, R. Casadio, R. da Rocha, A. Sotomayor, *Eur. Phys. J. C* **78**, 122 (2018)

54. J. Ovalle, R. Casadio, *Beyond Einstein Gravity: The Minimal Geometric Deformation Approach in the Brane-World* (Springer Nature, Berlin, 2020)

55. J. Ovalle, *Phys. Lett. B* **788**, 213 (2019)

56. M.A. Habsi, S.K. Maurya, S.A. Badri et al., *Eur. Phys. J. C* **83**, 286 (2023)

57. S.K. Maurya, K.N. Singh, M. Govender, S. Ray, *Fortschr. Phys.* **2300023** (2023). <https://doi.org/10.1002/prop.202300023>

58. S.K. Maurya, R. Nag, *Eur. Phys. J. C* **82**, 48 (2022)

59. S.K. Maurya, A. Errehymy, R. Nag, M. Daoud, *Fortschr. Phys.* **70**(5), 2200041 (2022)

60. M. Sharif, A. Majid, *Chin. J. Phys.* **61**, 38–46 (2019)

61. Z. Yousaf, *Phys. Scr.* **95**(7), 075307 (2020)

62. H. Nazar, A.H. Alkhaldi, G. Abbas, M.R. Shahzad, *Int. J. Mod. Phys. A* **36**(31n32), 2150233 (2021)

63. Z. Yousaf, M.Z. Bhatti, K. Hassan, *Eur. Phys. J. Plus* **135**, 397 (2020)

64. M. Sharif, A. Majid, M.M.M. Nasir, *Int. J. Mod. Phys. A* **34**(32), 1950210 (2019)

65. M.Z. Bhatti, Z. Yousaf, S. Khan, *Int. J. Mod. Phys. D* **30**(13), 2150097 (2021)

66. M. Zubair, H. Azmat, *Phys. Dark Universe* **28**, 100531 (2020)

67. H. Azmat, M. Zubair, Z. Ahmad, *Ann. Phys.* **439**, 168769 (2022)

68. H. Azmat, M. Zubair, *Eur. Phys. J. Plus* **136**, 112 (2021)

69. M. Zubair, H. Azmat, E. Gudekli, A. Alhowaity, H. Hamam, *New Astron.* **100**, 101996 (2023)

70. S.K. Maurya, A. Errehymy, M. Govender et al., *Eur. Phys. J. C* **83**, 348 (2023)

71. Z. Yousaf, M.Z. Bhatti, T. Naseer, I. Ahmad, *Phys. Dark Universe* **29**, 100581 (2020)

72. Z. Yousaf, M.Z. Bhatti, T. Naseer, *Phys. Dark Universe* **28**, 100535 (2020)

73. M. Sharif, A. Majid, *Indian J. Phys.* **95**, 769–777 (2021)

74. M.K. Jasim et al., *Phys. Scr.* **98**, 045305 (2023)

75. K.R. Karmarkar, *Proc. Indian Acad. Sci. A* **27**, 56 (1948)

76. S. Ngubelanga, S. Maharaj, *Eur. Phys. J. Plus* **130**, 211 (2015)

77. S.D. Maharaj, D.K. Matondo, *New Astron.* **97**, 101852 (2022)

78. S. Thirukkanesh, F.C. Ragel, *Astrophys. Space Sci.* **354**, 415–420 (2014)

79. Y. Kim, C.H. Lee, I.J. Shin et al., *J. High Energ. Phys.* **2011**, 111 (2011)

80. L. Herrera, *Entropy* **23**, 802 (2021). <https://doi.org/10.3390/e23070802>

81. Z. Yousaf et al., *New Astron.* **84**, 101541 (2021)

82. J. Sanudo, A.F. Pacheco, *Phys. Lett. A* **373**, 807–810 (2009)

83. L. Bel, *Ann. Inst. Henri Poincaré* **17**, 37 (1961)

84. A.G.P. Gómez-Lobo, *Class. Quantum Gravity* **25**, 015006 (2007)

85. L. Herrera, J. Ospino, A. Di Prisco, E. Fuenmayor, O. Troconis, *Phys. Rev. D* **79**, 064025–12 (2009)

86. C. Arias et al., *Ann. Phys.* **436**, 168671 (2022)

87. S.K. Maurya, M. Govender, G. Mustafa et al., *Eur. Phys. J. C* **82**, 1006 (2022)

88. E. Contreras, E. Fuenmayor, G. Abellán, *Eur. Phys. J. C* **82**, 187 (2022)

89. J. Andrade, *Eur. Phys. J. C* **82**, 617 (2022)

90. R. Casadio, E. Contreras, J. Ovalle et al., *Eur. Phys. J. C* **79**, 826 (2019)

91. P. León, C. LasHeras, *Eur. Phys. J. C* **83**, 260 (2023)

92. B. Dayanandan et al., *SSRN* (2023). <https://doi.org/10.2139/ssrn.4350104>

93. A. Rincón, G. Panotopoulos, I. Lopes, *Eur. Phys. J. C* **83**, 116 (2023)

94. A. Rincón, G. Panotopoulos, I. Lopes, *Universe* **9**(2), 72 (2023)

95. J. Andrade, *Eur. Phys. J. C* **82**, 266 (2022)

96. E. Contreras, Z. Stuchlik, *Eur. Phys. J. C* **82**, 706 (2022)

97. S.K. Maurya, A. Errehymy, M.K. Jasim et al., *Eur. Phys. J. C* **82**, 1173 (2022)

98. M.R. Finch, J.E.F. Skea, *Class. Quantum Gravity* **6**, 467 (1989)

99. B.V. Ivanov, *Eur. Phys. J. C* **77**, 738 (2017)

100. B.V. Ivanov, *Phys. Rev. D* **65**(10), 104011 (2002)

101. H. Abreu, H. Hernández, L.A. Núñez, *Class. Quantum Gravity* **24**(18), 4631 (2007)

102. C.A. Kolassis et al., *Class. Quantum Gravity* **5**, 1329 (1988)

103. H. Bondi, Proc. R. Soc. Lond. Ser. A Math. Phys. Eng. Sci. **282**(1390), 303–317 (1964). <https://doi.org/10.1098/rspa.1964.0234>
104. K.S. Thorne, *Astrophys. J.* **144**, 201–205 (1966)
105. A. Kovetz, *Zeitschrift für Astrophysik* **66**, 446 (1967)
106. H. Hernández, L. Núñez, A. Vázquez, *Eur. Phys. J. C* **78**, 883 (2018)
107. F. Tello-Ortiz, S.K. Maurya, Y. Gomez-Leyton, *Phys. J. C* **80**, 324 (2020)
108. C.C. Moustakidis, *Gen. Relativ. Gravit.* **49**, 68 (2017)
109. S.K. Maurya, R. Nag, *Eur. Phys. J. Plus* **136**, 679 (2021)
110. L. Herrera, *Phys. Lett. A* **165**, 206 (1992)
111. A. Di Prisco, E. Fuenmayor, L. Herrera, V. Varela, *Phys. Lett. A* **195**, 23 (1994)
112. A. Di Prisco, L. Herrera, V. Varela, *Gen. Relativ. Gravit.* **29**, 1239 (1997)
113. L. Herrera, V. Varela, *Phys. Lett. A* **226**, 143 (1997)
114. J. Mimoso, M. Le Delliou, F. Mena, *Phys. Rev. D* **81**, 123514 (2010)
115. M. Le Delliou, J. Mimoso, F. Mena, M. Fontanini, D. Guariento, E. Abdalla, *Phys. Rev. D* **88**, 027301 (2013)
116. J. Mimoso, M. Le Delliou, F. Mena, *Phys. Rev. D* **88**, 043501 (2013)
117. E. Contreras, E. Fuenmayor, *Phys. Rev. D* **103**(12), 124065 (2021)
118. P. León, E. Fuenmayor, E. Contreras, *Phys. Rev. D* **104**(4), 044053 (2021)
119. J. Andrade, E. Fuenmayor, E. Contreras, *Int. J. Mod. Phys. D* **31**, 2250093 (2022)